Surfaces Inspired by the *Nepenthes* Peristome for Unidirectional Liquid Transport

Pengfei Zhang, Liwen Zhang, Huawei Chen, Zhichao Dong,* and Deyuan Zhang*

The slippery peristome of the pitcher plant *Nepenthes* has attracted much attention due to its unique function for preying on insects. Recent findings on the peristome surface of *Nepenthes alata* demonstrate a fast and continuous unidirectional liquid transport, which is enabled by the combination of a pinning effect at the sharp edges and a capillary rise in the wedge, deriving from the multiscale structure, which provides inspiration for designing and fabricating functional surfaces for unidirectional liquid transport. Developments in the fabrication methods of peristome-inspired surfaces and control methods for liquid transport are summarized. Both potential applications in the fields of microfluidic devices, biomedicine, and mechanical engineering and directions for further research in the future are discussed.

1. Introduction

Many natural systems have evolved into functional surfaces to achieve water transport for survival,[1–10] for example, the back of desert beetles,[1] shorebird beaks,[3] spider silk,[5] and cactus spines.[6] Without energy input, these biological surfaces can harness the movement of water through their unique structural features and chemical composition,[11–13] which gives inspiration for designing and fabricating functional surfaces and materials with wide applications in fields including antifogging and fog-collection,[14–16] microfluidic devices,[17–21] lubrication,[22,23] and liquid transport.[24–27] One-dimensional materials for unidirectional liquid transport, inspired by spider silk and cactus spines, have attracted major research interest in the last few years.[5,6,28] The developed fabrication and functionalization methods make great contribution to their practical applications.[29–33] However, the diversity and development of two-dimensional surfaces for liquid transport have gradually encountered bottlenecks.[34–39] Liquid transport on surfaces with chemical patterns or gradients, inspired by desert beetles etc., is confined to a small amplitude with a slow moving speed.[34,40–42] The design and fabrication of functional surfaces with fast and continuous liquid transport ability has received increasing attention.

The carnivorous pitcher plant, *Nepenthes*, can capture insects to meet their fundamental nutrient needs through their peristome.[43,44] The peristome can be completely wetted by water and then form a slippery liquid film, which induces insects to "aquaplane" on it.[45] This gives inspiration for designing well-known slippery surfaces.[46–51] Recently, it was found that the liquid-film formation was caused by continuous water transport on the peristome.[10] The multiscale surface structure of the peristome can optimize and enhance capillary rise along the spreading direction, and results in fast water transport. In the reverse direction, however, water flow is pinned in place by the sharp edges. Herein, we will briefly review the progress in studies on surfaces inspired by the *Nepenthes* peristome, mainly introducing the developed fabrication methods, control over the unidirectional liquid transport, and their potential applications.

2. Unidirectional Water Transport on the Peristome of *Nepenthes alata*

The slippery peristome of *Nepenthes* (**Figure 1**a), completely wetted by water, has been considered as the source of the insect-capture function. However, the question of how the water flows and then forms a uniform liquid film on the peristome has long been neglected. A recent study demonstrated that there is a unidirectional water-transport process after a water droplet is dropped on the peristome surface.[10] The unidirectional transport enables the droplet to form a uniform liquid film, which contributes to the slippery function. This unique fluid flow is caused by the multiscale structure. There is a two-order hierarchy of parallel microgrooves, with about ten second-order microgrooves scattering along the first-order microgrooves (Figure 1b,c). Along the second-order microgrooves, there are many anisotropic overlapping and arch-shaped microcavities, with the tops of the arches pointing toward the outer side. The microcavity is closed and has a sharp arc-shaped edge (approximately 2° to 8°). Besides, the sides of each microcavity form a gradient wedge angle (approximately 90° at the bottom of

Dr. P. Zhang, Dr. L. Zhang, Prof. H. Chen, Prof. D. Zhang
School of Mechanical Engineering and Automation
Beihang University
Beijing 100191, China
E-mail: chenhw75@buaa.edu.cn
Dr. Z. Dong
CAS Key Laboratory of Bio-inspired Materials and Interfacial Science
CAS Center for Excellence in Nanoscience
Technical Institute of Physics and Chemistry
Chinese Academy of Sciences
Beijing 100190, China
E-mail: dongzhichao@iccas.ac.cn
The ORCID identification number(s) for the author(s) of this article can be found under https://doi.org/10.1002/adma.201702995.

DOI: 10.1002/adma.201702995

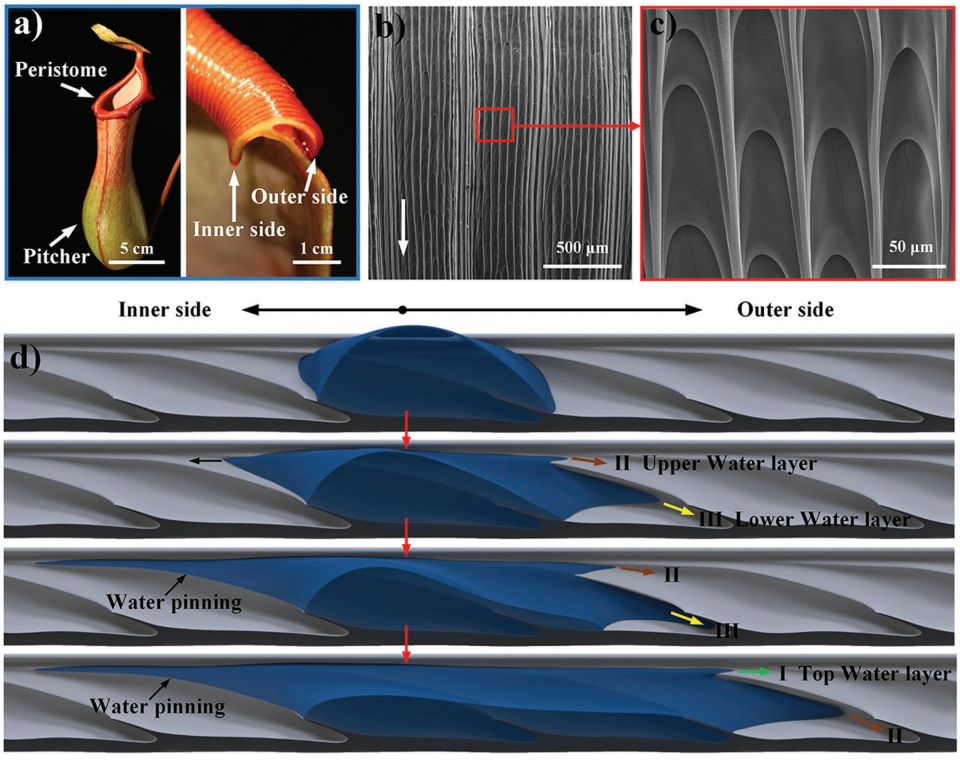

Figure 1. a) Optical images of a pitcher of *Nepenthes alata* (left) and its cross-section (right). b,c) SEM image of the peristome surface and its magnified image showing two-order microgrooves and periodic duck-billed microcavities scattering along the second-order microgroove. The arrow in (b) shows the direction toward the inner side. d) Three-dimensional illustration of the water-transport process. A strong water rise induced by the gradient wedge of the overlapping microcavities results in continuous water transport toward the outer side. Water pinning at the sharp edge prevents water flowing toward the inner side. Reproduced with permission.[10] Copyright 2016, Nature Publishing Group.

the microcavity to roughly 28° at the top). In conjunction with the superhydrophilicity, which itself has no power to drive the liquid flow unidirectionally but is necessary, these structural features result in unidirectional water transport.

The unidirectional transport can be explained from two aspects, that is, toward the inner side and toward the outer side. Because of the sharp edge of the microcavity, according to the Gibbs' inequality,[52] the water spreading toward the inner side tends to be pinned at the edge. Toward the outer side, continuous water transport is generated by the overlapped filling of the microcavities. For water filling in a specific single microcavity, an enhanced capillary rise, a gradient Taylor rise,[53,54] induced by the gradient wedge corner of the microcavity, contributes to the fast liquid flow.[55–58] The water firstly quickly spreads along the wedge, then pushes out the air, and finally converges at the front of the microcavity. The overall continuous unidirectional water transport is illustrated in Figure 1d. Water pinning at the sharp edge prevents wetting from proceeding toward the inner side. Sequential filling of each microcavity achieves continuous water transport.

The highlights of this unique liquid transport movement are not only its unidirectional transport on the superhydrophilic surface, but also its utilization of the gradient Taylor rise to form fast transport, with a speed that is much greater than that reported in a previous study.[34] Inspired by these results, functional surfaces with the same structures as the peristome or peristome-mimetic structures can be designed and fabricated to achieve fast unidirectional liquid transport.

3. Fabrication of Peristome-Inspired Surfaces

3.1. Replica Molding Method

To fabricate a surface with the same structural features as the natural peristome is a short-cut to achieving fast and continuous unidirectional liquid transport. The replica molding method is an ideal choice.[59] Directly using the natural peristome as a template, an artificial poly(dimethylsiloxane) (PDMS) peristome can be obtained by two steps of replication (**Figure 2**a).[60] The artificial peristome has multiscale and three-dimensional structures of two-order microgrooves and overlapping microcavities, just like the natural peristome (Figure 2b,c). Fast, continuous, unidirectional liquid transport is successfully reproduced on the PDMS peristome when the liquid completely wets the surface. It is worth noting that a freezing process to decrease the surface stickiness of the casting material of PDMS should be performed before peeling the negative replica off the natural template; otherwise, the protruding structures on the negative replica would have severe deformation, which can result in the loss of the structural features. The major limitations of the replica molding method are the small size and curved shape of the final formed surface.

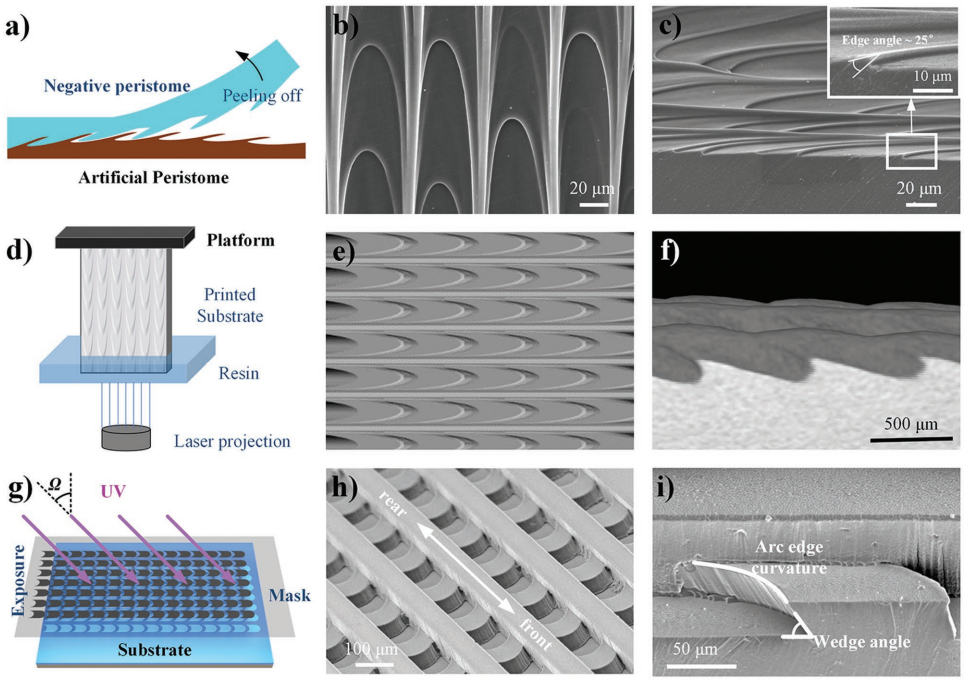

Figure 2. a) Schematic of replica molding method. b,c) SEM image of an artificial peristome surface by replica molding and its cross-section view. Reproduced with permission.[60] Copyright 2017, American Chemical Society. d) Schematic of stereolithography method. e,f) SEM image of peristome-mimetic surface by stereolithography and its cross-section view. Reproduced with permission.[61] Copyright 2016, Wiley-VCH. g) Schematic of the photolithography method. h,i) SEM image of peristome-mimetic surface by photolithography and its cross-section view. Reproduced with permission.[63] Copyright 2017, Royal Society of Chemistry.

Although its structure is the most ideal, the surface cannot be adjusted, which greatly limits the potential applications.

3.2. Stereolithography Method

To widen the application fields of peristome-mimetic surfaces, it is crucial to fabricate complicated three-dimensional structures on a large-area surface with an arbitrary shape on demand. Recently developed high-resolution stereolithography makes it possible (Figure 2d).[61] By extracting the structural parameters of the peristome structure, its three-dimensional data model is built. After inputting the data into the Stereolithography instrument, a biomimetic surface with a similar morphology to the peristome can be fabricated directly, as shown in Figure 2e,f. By changing surface energy of the biomimetic surface, liquids with different surface tensions and viscosities show unidirectional transport on the surface. This fabricated structure is bigger than that on the natural peristome and is favorable to be used for investigating the liquid-wetting mechanism on the structure by X-ray microscopy. In addition, three-dimensional materials with peristome-mimetic structures can be fabricated using this method, and this provides a new way of expanding its application areas such as microfluidic devices, high-resolution printing, and so on.

3.3. Photolithography Method

In fact, unidirectional water transport is mainly determined by the overlapping microcavities, together with the second-order microgrooves. It is also possible to achieve unidirectional liquid transport by fabricating simplified structures. We proposed a two-step UV photolithography method to fabricate the biomimetic surface with an inclined pit array along the microgrooves (Figure 2g).[62,63] First, an inclined pit array is fabricated by adjusting the UV source with an inclined incident angle through the arc patterns on the mask. Second, overlaid microgrooves with the same width as the pit array are fabricated by a second photolithography (Figure 2h). The prepared pit has an arc-shaped edge, which favors liquid pinning. The inclined side surface forms a wedge corner with the bottom surface of the pit and contributes to water spreading (Figure 2i). Thus, these anisotropic structures produce asymmetric liquid wetting and can harness the liquid to spread unidirectionally. Due to the controllability and high precision of this method, the prepared surface shows a great application potential in the field of microfluidic devices.

4. Control of Unidirectional Liquid Transport on Peristome-Inspired Surface

4.1. Intrinsic Wettability

It is worth noting that unidirectional liquid transport can be achieved by fabricating peristome-inspired surfaces using different methods, but how to control the liquid flow is also crucial for practical applications. The relationship between the unidirectional liquid transport and the surface wettability has been revealed by adjusting surface energy and liquid surface

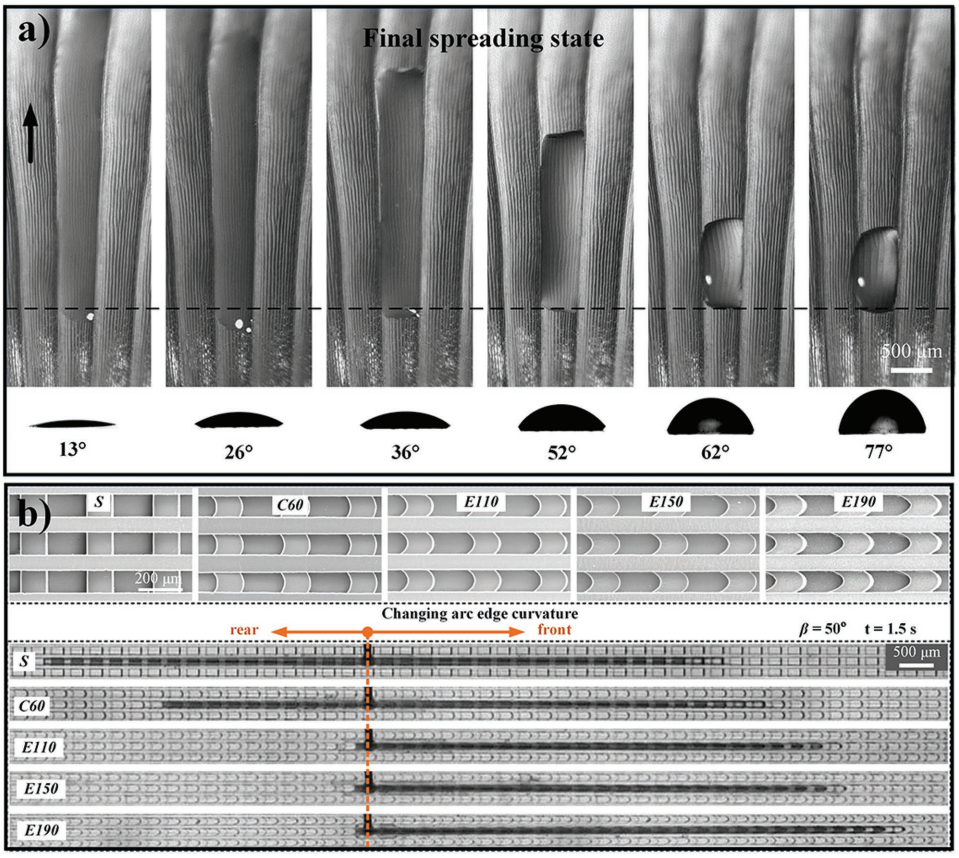

Figure 3. a) Final states of water spreading on PDMS peristomes with different surface energies (corresponding to the different intrinsic contact angles marked below), which shows that the water-spreading ability decreases with increasing intrinsic contact angle. Reproduced with permission.[60] Copyright 2017, American Chemical Society. The black arrow in (a) indicates the direction toward the outer side of the peristome. b) The final states of spreading of liquid ethanol on peristome-mimetic surfaces with different arc edge curvatures. Unidirectional liquid spreading occurs on a surface with an ellipse arc edge, and the spreading distance increases with the increase of the semi-major axis. Reproduced with permission.[63] Copyright 2017, Royal Society of Chemistry.

tension.[60] Artificial PDMS peristomes with different surface energies, corresponding to different intrinsic contact angles, are obtained by changing storage time in air after O_2-plasma treatment. Water-spreading experiments demonstrate that the unidirectional transport ability decreases with the decrease of surface energy (**Figure 3**a). Liquids with different surface tensions are obtained by choosing different ethanol aqueous solutions, and spreading experiments show that the unidirectional transport ability increases with the decrease of the surface tension. From the perspective of intrinsic wettability, these two experiments show the same result, that the unidirectional liquid-transport ability decreases with the increase of intrinsic contact angle, and they also have a similar threshold for unidirectional liquid transport, i.e., an intrinsic contact angle of 62–65°, approximately corresponding to the newly defined critical angle of 65°.[64,65] These findings are also found for other *Nepenthes*-inspired surfaces.[60] For example, on the peristome-mimetic surface fabricated by stereolithography, liquid ethanol and FC-72, which have intrinsic contact angles below 62–65° on a PDMS surface, show unidirectional liquid transport. Ethylene glycol, however, with an intrinsic contact angle of about 73° on a PDMS surface, does not show unidirectional transport. Thus, by tuning the intrinsic wettability of liquids on peristome-inspired surfaces, unidirectional liquid transport can be controlled.

4.2. Adjusting Structures

For a fixed surface with specific intrinsic wettability, adjusting the structures is another method to control the liquid transport. By investigating liquid spreading on the inclined pit arrays in the microgrooves, it was found that two structure parameters of arc edge curvature and wedge angle greatly impact the liquid transport.[63] As shown in Figure 3b, for a specific wedge angle of 50°, nearly no unidirectional liquid transport occurs with the straight edge (S) and circle arc edge (C); however, unidirectional liquid transport occurs with the ellipse arc edge (E). In addition, the unidirectional liquid transport ability increases with the increase of curvature. For a specific ellipse arc with a semi-major axis length of 190 μm (E190), the unidirectional liquid transport decreases with the increase of wedge angle, and liquid spreading toward the rear direction tends to be more and more evident when the wedge angle increases to above 70°. Therefore, it is concluded that the speed and distance of the unidirectional liquid transport

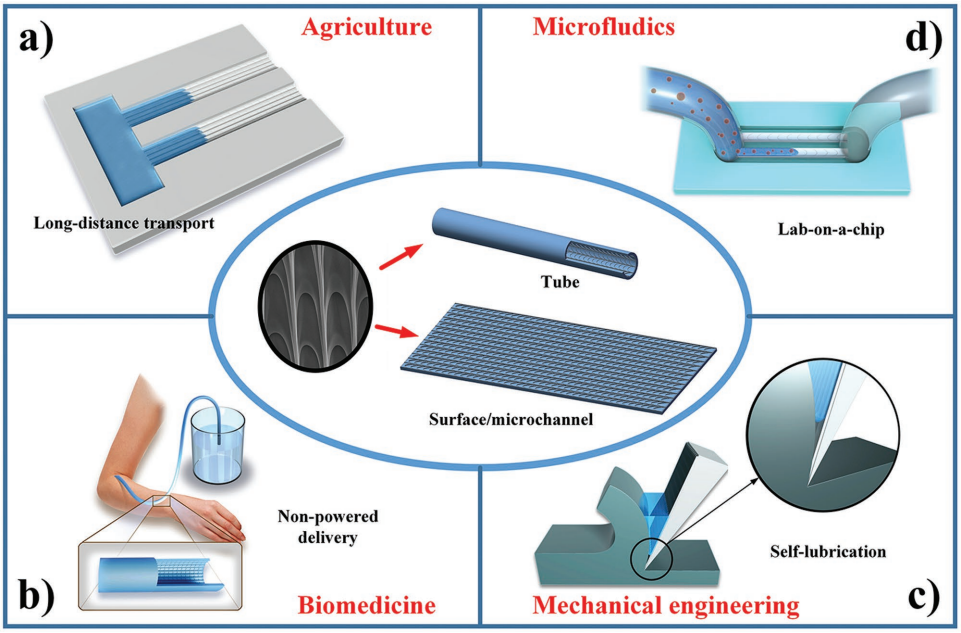

Figure 4. Schematics of potential applications of peristome-inspired surfaces. a) Channels with peristome-mimetic structures can be used for long-distance liquid transport, with potential in agricultural drip irrigation. b) Tubes with a peristome-mimetic inner surface make nonpowered delivery of microdrugs possible. c) Controllable unidirectional liquid transport of peristome-inspired surfaces may achieve self-lubrication, with wide applications in mechanical engineering, such as the self-lubrication of cutting tools. d) Peristome-mimetic structures with anisotropic liquid flow may find applications in microfluidics.

can be controlled by changing the inclined pit structure in the microgrooves.

5. Applications of Peristome-Inspired Surfaces

Previous studies of surfaces inspired by the *Nepenthes* peristome have mainly focused on structure fabrication and the control method. The mentioned applications were based on the straightforward unidirectional liquid-transport ability of the prepared surfaces. For example, peristome-mimetic surfaces were fabricated on a three-dimensional elevated spiral, and then the surface could transport the liquid upward.[61] These results demonstrate that peirstome-inspired surfaces have the potential for liquid transport on an inclined surface. For further applications, the surfaces have the potential to transport water for agricultural drip irrigation over a long distance (**Figure 4**a). If peristome-inspired structures are prepared on the inner wall of a tube, the tube will have the potential to transport liquid in a closed environment, implying applications in biomedicine such as in nonpowered delivery of microdrugs (Figure 4b).[66] Besides, because the liquid-transport ability can be controlled by manipulating the surface wettability, smart peristome-inspired surfaces can be prepared by constructing stimulus-responsive materials on the surfaces.[60,67,68] This will result in a controllable liquid flow on the surface, showing wide applications in mechanical engineering, including in controllable self-lubrication (Figure 4c), and heat or mass transfer.[69] In addition, one of the important applications of peristome-mimetic structures could be in microfluidics,[70] and the unidirectional liquid transport on the biomimetic structure in channels could be used for smart and controllable microfluidic devices (Figure 4d), for example, the lab-on-a-chip. The developed preparation and control method have constructed the platform for further research in applications, and its huge potential should be delivered in the near future.

6. Conclusions and Outlook

Here, we give a brief overview of the recent progress in the field of *Nepenthes*-peristome-inspired surfaces for unidirectional liquid transport. The finding of continuous water transport forming a slippery liquid film on the peristome surface of *Nepenthes alata* gives a new way to design two-dimensional surfaces to achieve fast unidirectional liquid transport. The multiscale structure of the peristome can be fabricated by several methods including replica molding, Stereolithography, and photolithography. By manipulating the wettability between the liquid and the surface and by changing the structure parameters, the unidirectional liquid transport can be successfully controlled. These recently developed fabrication and control methods for surfaces inspired by the *Nepenthes* peristome will have wider applications in the fields of microfluidic devices, biomedicine, mechanical engineering, and agriculture.

In addition, spontaneous liquid unidirectional transport makes it possible to achieve the dynamic formation and control of a sliding liquid layer, known as slippery surfaces, which are well-developed in recent years, and constructs a bridge between the liquid transport and the slippery surfaces. As a result, this new strategy will be able to be applied to a wide range of interfaces between liquids and solid materials in the future. With

the help of the enormous development of smart-responsive interfacial materials, researchers nowadays have greater opportunities to devise drop-motion-manipulation systems with smart-responsive properties. We envision that the future of liquid-unidirectional-motion systems will be promoted to a direction with biocompatible, smart, features integrated with multiple functions.

Acknowledgements

P.Z. and L.Z. contributed equally to this work. This work was supported by the Major project of the National Natural Science Foundation of China (No. 51290292) and the Academic Excellence Foundation of BUAA for PhD Students.

Conflict of Interest

The authors declare no conflict of interest.

Keywords

bioinspired surfaces, *Nepenthes alata*, peristome-mimetic surfaces, unidirectional liquid transport

Received: May 29, 2017
Revised: June 23, 2017
Published online: August 7, 2017

[1] A. R. Parker, C. R. Lawrence, *Nature* **2001**, *414*, 33.
[2] L. Feng, S. Li, Y. Li, H. Li, L. Zhang, J. Zhai, Y. Song, B. Liu, L. Jiang, D. Zhu, *Adv. Mater.* **2002**, *14*, 1857.
[3] M. Prakash, D. Quere, J. W. Bush, *Science* **2008**, *320*, 931.
[4] P. M. Reis, S. Jung, J. M. Aristoff, R. Stocker, *Science* **2010**, *330*, 1231.
[5] Y. Zheng, H. Bai, Z. Huang, X. Tian, F. Q. Nie, Y. Zhao, J. Zhai, L. Jiang, *Nature* **2010**, *463*, 640.
[6] J. Ju, H. Bai, Y. Zheng, T. Zhao, R. Fang, L. Jiang, *Nat. Commun.* **2012**, *3*, 1247.
[7] D. Ishii, H. Horiguchi, Y. Hirai, H. Yabu, Y. Matsuo, K. Ijiro, K. Tsujii, T. Shimozawa, T. Hariyama, M. Shimomura, *Sci. Rep.* **2013**, *3*, 3024.
[8] T.-S. Wong, T. Sun, L. Feng, J. Aizenberg, *MRS Bull.* **2013**, *38*, 366.
[9] C. Liu, J. Ju, Y. Zheng, L. Jiang, *ACS Nano* **2014**, *8*, 1321.
[10] H. Chen, P. Zhang, L. Zhang, H. Liu, Y. Jiang, D. Zhang, Z. Han, L. Jiang, *Nature* **2016**, *532*, 85.
[11] M. K. Chaudhury, G. M. Whitesides, *Science* **1992**, *256*, 1539.
[12] É. Lorenceau, D. Quéré, *J. Fluid Mech.* **2004**, *510*, 29.
[13] M. W. Denny, *Science* **2008**, *320*, 886.
[14] F. C. Cebeci, Z. Wu, L. Zhai, R. E. Cohen, M. F. Rubner, *Langmuir* **2006**, *22*, 2856.
[15] K.-C. Park, P. Kim, A. Grinthal, N. He, D. Fox, J. C. Weaver, J. Aizenberg, *Nature* **2016**, *531*, 78.
[16] Z. Han, Z. Mu, B. Li, Z. Wang, J. Zhang, S. Niu, L. Ren, *ACS Nano* **2016**, *10*, 8591.
[17] T. Wang, H. Chen, K. Liu, S. Wang, P. Xue, Y. Yu, P. Ge, J. Zhang, B. Yang, *ACS Appl. Mater. Interfaces* **2015**, *7*, 376.
[18] J. A. Lv, Y. Liu, J. Wei, E. Chen, L. Qin, Y. Yu, *Nature* **2016**, *537*, 179.
[19] S. Huang, J. Song, Y. Lu, C. Lv, H. Zheng, X. Liu, Z. Jin, D. Zhao, C. J. Carmalt, I. P. Parkin, *J. Mater. Chem. A* **2016**, *4*, 13771.
[20] Y. Yu, F. Fu, L. Shang, Y. Cheng, Z. Gu, Y. Zhao, *Adv. Mater.* **2017**, *29*, 1605765.
[21] T. Zhou, J. Yang, D. Zhu, J. Zheng, S. Handschuh-Wang, X. Zhou, J. Zhang, Y. Liu, Z. Liu, C. He, X. Zhou, *Adv. Sci.* **2017**, *4*, 1700028.
[22] B. R. Solomon, K. S. Khalil, K. K. Varanasi, *Langmuir* **2014**, *30*, 10970.
[23] P. Zhang, H. Chen, L. Zhang, Y. Zhang, D. Zhang, L. Jiang, *J. Mater. Chem. A* **2016**, *4*, 12212.
[24] Y. Cui, D. Li, H. Bai, *Ind. Eng. Chem. Res.* **2017**, *56*, 4887.
[25] X. C. Chen, K. F. Ren, J. Wang, W. X. Lei, J. Ji, *ACS Appl. Mater. Interfaces* **2017**, *9*, 1959.
[26] S. Deng, W. Shang, S. Feng, S. Zhu, Y. Xing, D. Li, Y. Hou, Y. Zheng, *Sci. Rep.* **2017**, *7*, 45687.
[27] M. Tenjimbayashi, M. Higashi, T. Yamazaki, I. Takenaka, T. Matsubayashi, T. Moriya, M. Komine, R. Yoshikawa, K. Manabe, S. Shiratori, *ACS Appl. Mater. Interfaces Interfaces* **2017**, *9*, 10371.
[28] J. Ju, Y. Zheng, L. Jiang, *Acc. Chem. Res.* **2014**, *47*, 2342.
[29] H. Bai, X. Tian, Y. Zheng, J. Ju, Y. Zhao, L. Jiang, *Adv. Mater.* **2010**, *22*, 5521.
[30] E. Kang, G. S. Jeong, Y. Y. Choi, K. H. Lee, A. Khademhosseini, S.-H. Lee, *Nat. Mater.* **2011**, *10*, 877.
[31] N. C. Tansil, Y. Li, C. P. Teng, S. Zhang, K. Y. Win, X. Chen, X. Y. Liu, M. Y. Han, *Adv. Mater.* **2011**, *23*, 1463.
[32] H. Bai, J. Ju, Y. Zheng, L. Jiang, *Adv. Mater.* **2012**, *24*, 2786.
[33] K. Li, J. Ju, Z. Xue, J. Ma, L. Feng, S. Gao, L. Jiang, *Nat. Commun.* **2013**, *4*, 2276.
[34] K. H. Chu, R. Xiao, E. N. Wang, *Nat. Mater.* **2010**, *9*, 413.
[35] N. A. Malvadkar, M. J. Hancock, K. Sekeroglu, W. J. Dressick, M. C. Demirel, *Nat. Mater.* **2010**, *9*, 1023.
[36] W. Wu, L. Cheng, S. Bai, Z. L. Wang, Y. Qin, *Adv. Mater.* **2012**, *24*, 817.
[37] Y. Hou, B. Xue, S. Guan, S. Feng, Z. Geng, X. Sui, J. Lu, L. Gao, L. Jiang, *NPG Asia Mater.* **2013**, *5*, e77.
[38] C. Q. Lai, W. K. Choi, *Adv. Mater. Interfaces* **2015**, *2*, 1400444.
[39] L. Wang, W. Shi, Y. Hou, M. Zhang, S. Feng, Y. Zheng, *Adv. Mater. Interfaces* **2015**, *2*, 1500040.
[40] M. Zhang, L. Wang, Y. Hou, W. Shi, S. Feng, Y. Zheng, *Adv. Mater.* **2015**, *27*, 5057.
[41] M. J. Hancock, K. Sekeroglu, M. C. Demirel, *Adv. Funct. Mater.* **2012**, *22*, 2223.
[42] H. Wu, K. Zhu, B. Cao, Z. Zhang, B. Wu, L. Liang, G. Chai, A. Liu, *Soft Matter* **2017**, *13*, 2995.
[43] U. Bauer, W. Federle, *Plant Signaling Behav.* **2009**, *4*, 1019.
[44] J. A. Moran, C. M. Clarke, *Plant Signaling Behav.* **2010**, *5*, 644.
[45] H. F. Bohn, W. Federle, *Proc. Natl. Acad. Sci. USA* **2004**, *101*, 14138.
[46] T. S. Wong, S. H. Kang, S. K. Tang, E. J. Smythe, B. D. Hatton, A. Grinthal, J. Aizenberg, *Nature* **2011**, *477*, 443.
[47] X. Yao, Y. Hu, A. Grinthal, T. S. Wong, L. Mahadevan, J. Aizenberg, *Nat. Mater.* **2013**, *12*, 529.
[48] P. Zhang, H. Chen, L. Zhang, T. Ran, D. Zhang, *Appl. Surf. Sci.* **2015**, *355*, 1083.
[49] C. Liu, H. Ding, Z. Wu, B. Gao, F. Fu, L. Shang, Z. Gu, Y. Zhao, *Adv. Funct. Mater.* **2016**, *26*, 7937.
[50] J. Jiang, H. Zhang, W. He, T. Li, H. Li, P. Liu, M. Liu, Z. Wang, Z. Wang, X. Yao, *ACS Appl. Mater. Interfaces* **2017**, *9*, 6599.
[51] J. Zhang, C. Gu, J. Tu, *ACS Appl. Mater. Interfaces* **2017**, *9*, 11247.
[52] J. F. Oliver, C. Huh, S. G. Mason, *J. Colloid Interface Sci.* **1977**, *59*, 568.
[53] B. Taylor, *Philos. Trans. R. Soc. London* **1712**, *27*, 538.
[54] F. Hauksbee, *Philos. Trans. R. Soc. London* **1712**, *27*, 539.
[55] P. Concus, R. Finn, *Proc. Natl. Acad. Sci. USA* **1969**, *63*, 292.
[56] R. Finn, *Not. Am. Math. Soc.* **1999**, *46*, 770.
[57] F. J. Higuera, A. Medina, A. Linan, *Phys. Fluids* **2008**, *20*, 102102.

[58] A. Ponomarenko, D. Quéré, C. Clanet, *J. Fluid Mech.* **2011**, *666*, 146.
[59] M. H. Sun, C. X. Luo, L. P. Xu, H. Ji, Q. Ouyang, D. P. Yu, Y. Chen, *Langmuir* **2005**, *21*, 8978.
[60] P. Zhang, H. Chen, L. Li, H. Liu, G. Liu, L. Zhang, D. Zhang, L. Jiang, *ACS Appl. Mater. Interfaces* **2017**, *9*, 5645.
[61] C. Li, N. Li, X. Zhang, Z. Dong, H. Chen, L. Jiang, *Angew. Chem., Int. Ed.* **2016**, *55*, 14988; *Angew. Chem.* **2016**, *128*, 15097.
[62] H. Chen, L. Zhang, P. Zhang, D. Zhang, Z. Han, L. Jiang, *Small* **2017**, *13*, 1601676.
[63] H. Chen, L. Zhang, Y. Zhang, P. Zhang, D. Zhang, L. Jiang, *J. Mater. Chem. A* **2017**, *5*, 6914.
[64] E. A. Vogler, *Adv. Colloid Interface Sci.* **1998**, *74*, 69.
[65] Y. Tian, L. Jiang, *Nat. Mater.* **2013**, *12*, 291.
[66] S. Herrlich, S. Spieth, S. Messner, R. Zengerle, *Adv. Drug Delivery Rev.* **2012**, *64*, 1617.
[67] T. Sun, G. Wang, L. Feng, B. Liu, Y. Ma, L. Jiang, D. Zhu, *Angew. Chem., Int. Ed.* **2004**, *43*, 357; *Angew. Chem.* **2004**, *116*, 361.
[68] X. Huang, Y. Sun, S. Soh, *Adv. Mater.* **2015**, *27*, 4062.
[69] H. J. Cho, D. J. Preston, Y. Zhu, E. N. Wang, *Nat. Rev. Mater.* **2016**, *2*, 16092.
[70] X. Hou, Y. S. Zhang, G. Trujillo-de Santiago, M. M. Alvarez, J. Ribas, S. J. Jonas, P. S. Weiss, A. M. Andrews, J. Aizenberg, A. Khademhosseini, *Nat. Rev. Mater.* **2017**, *2*, 17016.